NASA CONTRACTOR REPORT

A RESEARCH STUDY FOR THE PRELIMINARY DEFINITION OF AN AEROPHYSICS FREE-FLIGHT LABORATORY FACILITY

Thomas N. Canning

Eloret Institute
1178 Maraschino Drive
Sunnyvale CA 94087

Prepared for
Ames Research Center
under Cooperative Agreement NCC2-504

National Aeronautics and
Space Administration

Ames Research Center
Moffett Field, California 94035

NASA CONTRACTOR REPORT

A RESEARCH STUDY FOR THE PRELIMINARY DEFINITION OF AN AEROPHYSICS FREE-FLIGHT LABORATORY FACILITY

Thomas N. Canning

CONTRACT NAS2-
NCC2-504

NASA

1. Report No.	2. Government Accession No.	3. Recipient's Catalog No.

4. Title and Subtitle	5. Report Date
A Research Study for the Preliminary Definition of an Aerophysics Free-Flight Laboratory Facility	January, 1989
	6. Performing Organization Code
7. Author(s)	8. Performing Organization Report No.
Thomas N. Canning	
	10. Work Unit No.
9. Performing Organization Name and Address	
Eloret Institute 1178 Maraschino Drive Sunnyvale CA 94087	11. Contract or Grant No. NCC2-504
	13. Type of Report and Period Covered
12. Sponsoring Agency Name and Address	10-01-87 - 12-31-88
National Aeronautics and Space Administr. Washington, D.C. 20456	14. Sponsoring Agency Code

15. Supplementary Notes

Point of Contact: J.O. Arnold, 229-3 NASA Ames Research Center, Moffett Field, CA 94035

16. Abstract

A renewed interest in hypervelocity vehicles requires an increase in our knowledge of aerodynamic phenomena. Tests conducted with ground-based facilities can be used both to better understand the physics of hypervelocity flight, and to calibrate and validate computer codes designed to predict vehicle performance in the hypervelocity environment. This research reviews the requirements for aerothermodynamic testing and discusses the ballistic range and its capabilities. Examples of the kinds of testing performed in typical high performance ballistic ranges are described. We draw heavily on experience obtained in the ballistics facilities at NASA Ames Research Center, Moffett Field, California. Prospects for improving the capabilities of the ballistic range by using advanced instrumentation are discussed. Finally, recent developments in gun technology and their application to extend the capability of the ballistic range are summarized.

17. Key Words (Suggested by Author(s))	18. Distribution Statement
Hypervelocity Vehicles Aerothermodynamic Testing Ballistic Range Gun Technology	Unclassified, Unlimited

19. Security Classif. (of this report)	20. Security Classif. (of this page)	21. No. of Pages	22. Price*
Unclassified	Unclassified	15	

*For sale by the National Technical Information Service, Springfield, Virginia 22161

A RESEARCH STUDY FOR THE PRELIMINARY DEFINITION OF AN AEROPHYSICS FREE-FLIGHT LABORATORY FACILITY

Final Technical Report

for
Cooperative Agreement NCC2-504

for the period
October 1, 1987 - December 31, 1988

Submitted to

National Aeronautics and Space Administration
Ames Research Center
Moffett Field, California 94035

Thermosciences Division
Dr. James O. Arnold
Chief and Technical Monitor

Prepared by

ELORET INSTITUTE
1178 Maraschino Drive
Sunnyvale, CA 94087
Phone: 408 730-8422 and 415 493-4710
Telefax: 408 730-1441
K. Heinemann, President and Grant Administrator
Thomas Canning, Principal Investigator

25 January, 1989

Research activities entitled "A Research Study for the Preliminary Definition of an Aerophysics Free-Flight Laboratory Facility" were conducted during the period 1 October, 1987, through 31 December, 1988 at the Thermosciences Division of NASA Ames Research Center. Principal Investigator was Thomas Canning, NASA Technical Monitor was Dr. James O. Arnold.

The results of this study are described in AIAA report No. 88-2015, which is made part of this final report.

THE BALLISTIC RANGE AND AEROTHERMODYNAMIC TESTING

A. W. Strawa* and G. T. Chapman,†
NASA Ames Research Center, Moffett Field, CA 94035

T. N. Canning‡
Eloret Institute, Sunnyvale, CA 94087

J. O. Arnold§
NASA Ames Research Center, Moffett Field, CA 94035

Abstract

A renewed interest in hypervelocity vehicles requires an increase in our knowledge of aerothermodynamic phenomena. Tests conducted in our ground-based facilities can be used both to better understand the physics of hypervelocity flight, and to calibrate and validate computer codes designed to predict vehicle performance in the hypervelocity environment. This paper reviews the requirements for aerothermodynamic testing and discusses the ballistic range and its capabilities. Examples of the kinds of testing performed in typical high-performance ballistic ranges are described; we draw heavily on experience obtained in the ballistics facilities at NASA Ames. Prospects for improving the capabilities of the ballistic range by using advanced instrumentation are discussed. Finally, recent developments in gun technology and their application to extend the capability of the ballistic range are summarized.

Introduction

In the last several years, there has been a resurgence of interest in hypervelocity flight. Several studies, most notably the Paine Commission Report,[1] call for a renewed initiative in space exploration. Its goals include the development of a space station, and colonization of the moon, as well as unmanned and manned exploration of Mars. To accomplish these goals, space vehicles must be developed that maximize payload mass ratios (the ratio of payload to total mass). Rather than using retrorockets to accomplish velocity changes, it will be necessary to use the upper atmosphere to aerobrake and aeromaneuver. Consequently, these missions require a much improved knowledge of hypervelocity flight, particularly in the area of aerothermodynamics. NASA has implemented the Civilian Space Technology Initiative (CSTI) and is advocating the Pathfinder Program to make these plans a reality. Further, the Office of Science and Technology Policy concluded, from an aeronautics point of view, that there is a need for enhanced hypersonic capabilities with airbreathing propulsion.[2] Programs currently under way include the National Aerospace Plane (NASP),[3] which is designed to improve our technology base in hypersonic flight and propulsion, and NASA's Aeroassisted Flight Experiment[4,5] (a part of CSTI), which is designed to improve our technology base for Aeroassisted Orbital Transfer Vehicles (AOTV). Artists' conceptions of these vehicles are illustrated in Fig. 1. The body on the left of the figure is a low L/D vehicle of the type that will be used for orbital transfer as well as for missions which require entry into extraterrestrial atmospheres and return to Earth, such as a Mars sample-return mission. The vehicle on the right is a high L/D airbreather, typical of what might be used for horizontal takeoff and landing, and would have a single-stage-to-orbit capability. Understanding the phenomena involved and developing these vehicles will require heavy use of our ground-based facilities, flight research, and computational fluid dynamics (CFD).

In the future, CFD will be used in vehicle design to a much greater extent than in the past. This is the result of the rapid development of CFD methodology, the large increase in computational power that has become available in the last 10 years, and the fact that ground-based test facilities cannot test all aspects of the flight environment experienced by future vehicles. The CFD codes will need to be verified by experiments. This will require more detailed tests and add to the work load in our ground-based facilities.

This paper reviews the aerothermodynamic requirements that these new missions and design methodologies require. The ballistic-range capabilities will then be examined in detail. Examples of the kinds of testing performed in typical high-performance ballistic ranges are described; we draw heavily on experience obtained in the ballistics facilities at NASA Ames. Finally, we discuss improvements needed in our existing facilities to meet the aerothermodynamic requirements, including new instrumentation and larger and faster launchers.

Aerothermodynamic Requirements

The flight environment of the missions mentioned earlier is shown in Fig. 2. The boundaries

---

*Research Scientist. Member AIAA.
†Senior Staff Scientist. Associate Fellow AIAA.
‡Senior Research Scientist.
§Division Chief, Thermophysics Division.

at which chemical and thermodynamic phenomena begin to be important are also shown. It can be seen that NASA's new missions extend the range of aerothermodynamic requirements. Nearly all of the mission profiles occur where there are significant amounts of oxygen and nitrogen dissociation. The higher velocity missions (for example, the Mars sample-return) also encounter significant amounts of ionization. The airbreathing NASP vehicle flies well beyond the region of our present experience and understanding of airbreathing propulsion as typified by the Concorde mission profile in the lower left corner of the chart. The lower boundary of the NASP flight envelope is the leg from takeoff to orbit and occurs at a very high dynamic pressure in order to provide adequate oxygen for the engine. This results in very high Reynolds numbers and, hence, boundary-layer transition and turbulent flow, which causes high drag and heat transfer. All of the vehicles spend time at very high altitude and encounter significant amounts of chemical and thermodynamic nonequilibrium. This is particularly true of the AOTVs, which spend nearly their entire flight life in this domain.

Some of the important aerothermodynamic requirements are now described. First, aerodynamic forces and moments, including the effects of control surfaces, must be known and understood. These must take into account the various fluid dynamic and chemical processes that occur under the appropriate flight conditions. This will include the special aerodynamic problems associated with the integration of the propulsion system into vehicles like the NASP. Here, not only the chemical processes of the external flow, but those associated with the power plant must be considered.

The second major requirement is a knowledge of the heat transfer that the vehicle will experience. This includes convective and radiative heat transfer, again under the extreme conditions of the various flight profiles. The items mentioned so far have been overall design-related issues, but their resolution will require detailed information about the basic phenomena that occur in these flight environments.

The four most significant phenomena are: the real-gas chemical effects; boundary-layer transition and turbulence; combustion for the airbreathing vehicles; and specific flow structures such as shock waves, shear layers, separation, vortex flows, and wakes. Finally, once the relevant phenomena have been understood, they must be incorporated into the CFD codes that will be used to design these vehicles and the codes then must be validated. This requires different types of data than those needed to understand the underlying physics. Meeting all of these requirements with the present available ground-based facilities will be difficult. The ballistic range has the ability to meet many of these requirements and its unique capabilities will be discussed next.

Ballistic-Range Characteristics

Present high-performance ballistic ranges have a two-stage light-gas gun, which is used to launch the model, a tank in which to separate the sabot from the model and eliminate gun gases, and a test section where the major portion of the instrumentation is located. (The sabot is used to encase the model in the launch tube and to help support the model during the high acceleration loads during launch. After launch, the sabot pieces are separated from the model, usually by aerodynamic forces, and the model is free to travel down the test section.) A schematic of a typical ballistic facility, the Hypersonic Free-Flight Aerodynamic Facility (HFFAF) at NASA Ames, is shown in Fig. 3. (A complete description of the range and ballistic range technology can be found in Ref. 6.) The HFFAF also has a counterflow capability. A large shock tube (shown in Fig. 3a) is used to generate a Mach 7 air flow through the test section in the opposite direction of the model flight to increase the relative Mach number. Besides the facilities at NASA Ames, there are very few ballistic facilities suitable for aerothermodynamic testing. One of these is at Arnold Engineering Development Center (AEDC) at Arnold Air Force Station, TN. A very wide assortment of models have been launched in these ballistic facilities. Some of the models launched in the Ames range are shown in Fig. 4.

The envelope of test conditions for the HFFAF is shown in Fig. 5 superimposed on some of the flight regimes of interest. (The length scales chosen for the Boost-Glide Vehicle (BGV), the Transatmospheric Vehicle (TAV), and the Aeroassisted Flight Experiment (AFE) were 30 m, while the length scale for the Space Transportation System (STS) was 22 m.) This is very typical of other high-performance ballistic ranges. It can be seen that the ballistic range covers a significant portion of the missions shown. A wide range of Mach and Reynolds numbers (M = 0.2 to 22, 30 with counterflow, and Re = 250 to 3×10^7) are possible. Free-stream chemical conditions equivalent to flight are achieved and there is very little free-stream flow disturbance. The test gas can be readily changed to any nontoxic gas (limited volumes of toxic gases). Also shown for comparison are other types of facilities.

Despite the wide simulation capability of the ballistic range, data acquisition can be a problem. With present guns, the models used are relatively small and simple. Complex models can be flown, but they require gentle launches and, in most cases, they must not have lift at trim conditions. At the present time, all high speed data are acquired remotely. Typical data obtained at the HFFAF are described briefly to illustrate some of the tests that have been performed in ballistic ranges. A wide variety of tests have been conducted in ballistic ranges including determination of aerodynamic forces and moments, documentation of flow-field structures such as shock shapes,

free-shear layers and wakes, investigations of boundary-layer transition, heat transfer (convective and radiative), and studies of the effects of ablation materials.

In a ballistic range, aerodynamic coefficients are measured in the following manner. As the model travels in free-flight down the test section, model position, orientation, and time-of-flight are recorded on film and chronographs. A data-reduction routine fits the equations of motion to the measured trajectory data by using a least-squares procedure. This method of determining aerodynamic coefficients is unlike techniques used in conventional facilities and has caused some questions to be raised about the results obtained in the range. Range methodologies, however, are similar to the way in which data are obtained from flight experiments.

The data presented in Figs. 6 and 7 were taken in support of the Pioneer Venus mission, which entered the Venusian atmosphere in 1978, and the Galileo mission, which is scheduled to enter the Jovian atmosphere in the 1990s.[7] Figure 6 shows drag data obtained for the Pioneer Venus configuration over a wide range of Reynolds number, down to a Reynolds number of 250, based on model diameter. The importance of attaining drag data at these low Reynolds numbers is that the drag coefficient increases markedly as the slip-flow and free-molecular-flow regimes are approached. The drag coefficient increases continuously below a $Re = 10^6$, but the increase becomes most dramatic below $Re = 10^3$. A comparison of drag coefficient data for Mach numbers from 0.2 to 22 is shown in Fig. 7 for the Pioneer Venus and Galileo configurations.

Since many shadowgraph photos are taken for most ballistic range launches, a study of the flow structure can be carried out on nearly any test (except when the density is too low). Figure 8 shows a typical shadowgraph of an AOTV-like vehicle in flight.[7] The particular point of interest for this test was to determine whether the free-shear layer coming from the corner of the model would impinge on the afterbody and cause a region of high heat transfer. Other features shown in this figure are bow and wake shocks as well as the beginning of the wake flow. All of these features can be useful in CFD code validation, and accurate determinations of the bow shock stand-off distance are a good indicator of the state of the chemistry in the shock layer.

Shadowgraph pictures have also been used to study the transition to turbulence. Figure 9 shows an example of one such study, reported on in Ref. 8. The figure shows a shadowgraph of a model flying at a Mach number of 3.9 and a Reynolds number per inch of 2.2×10^6. Evidence of turbulent bursts are clearly seen in the shadowgraph. In order to properly study transition in the range several factors must be considered. The temperature of the surface should be known. From the distribution of temperatures on the model surface, the heating history and location of spatially stable boundary-layer transition can be inferred. Sudden increases in the surface temperature gradient along a streamline indicate the onset of transition, and the surface roughness of the model must be known accurately. Direct incident-light photographs of the model in flight should be made in order to determine if the model has suffered any damage during launch and to see if there is any evidence of ablation affecting the transition to turbulence. The "unit Reynolds number effect," which is inferred from tests in conventional wind tunnels, is believed to result from noise generated in the wind tunnel flow; the ballistic range provides a much lower ambient noise level. Whether or not this effect is important in the range is still an unanswered question.

Convective and radiative heat transfer have also been measured in the ballistic range. Results for stagnation-point heat transfer on a hemisphere at 12 km/sec are shown in Fig. 10.[9] The heat transfer was inferred from the time the surface material (aluminum or nickel) started to melt. This method had an accuracy of ±10%. Note that this is well within the scatter of the shock-tube data.

Measurements of emission from the gas caps formed about blunt ballistic range models have been used to deduce radiative properties for both equilibrium and nonequilibrium thermochemical layers. The instrumentation used in one approach consisted of broad band spectral radiometers whose construction and calibration are described in Ref. 10. The analysis, described in Ref. 11, involves several steps: spectral integration of the radiometer data, calculation of the effective volume of the radiating gas cap observed, determination of the radiation per unit volume for equilibrium gasses and the variation of nonequilibrium radiation with density and velocity as provided from the range measurements. This information was sufficient to allow a prediction of equilibrium and nonequilibrium radiative heat transfer to the forebody of the Apollo vehicle.

Spatial distributions of shock-layer emission also have been measured by nearly head-on observations of ballistic range models. Instrumentation consisted of a calibrated image converter camera or a scanning method which focused light from the shock layer onto a small aperture in front of a photomultiplier tube. Details are contained in Chapter 9 of Ref. 6.

A novel technique[12-14] has been used to obtain spatially integrated spectra from the radiating gas cap formed about blunt models flying in the ballistic range. A schematic of the scanning spectrometer reported in Ref. 13 is shown in Fig. 11. As the model flies through the field of view and in the focal plane of the collecting mirror, the luminous gas cap acts as a moving entrance slit, sweeping out the spectrum of the

shock-heated gas on the exit slit. The process is optically equivalent to the model being held stationary and the grating rotated to scan the spectrum. It is necessary that the gas cap be the principal source of radiation in the flow field, and this can be accomplished by carefully choosing the model materials. The spectrally resolved light from the gas cap passes through the exit slit of the spectrometer, falling upon a photon sensor whose output is recorded with an oscilloscope. The spectral resolution is set mainly by the geometry of the gas cap emission, the exit slit width and the reciprocal dispersion of the spectrometer. A recording obtained[14] with such a device is shown in the inset in Fig. 11. These data were obtained in a gas (then thought to be representative of the Martian atmosphere) under nonequilibrium shock-layer conditions at a velocity of 6.3 km/s. Work similar to this could provide CFD calibration data on equilibrium and nonequilibrium shock layer flows.

Future Ballistic-Facility Needs

The ballistic range offers many advantages in the testing of hypersonic vehicles. However, the flight environment of future missions will stretch the simulation capabilities of existing facilities, and CFD validation needs will require data not presently obtained in the ballistic range. Many of the questions concerning aerothermodynamic phenomena can be answered in our existing ranges by adapting additional diagnostic techniques to the ballistic range. Larger models will be required to improve the quality of data and to allow the use of onboard instrumentation. In some cases, proper simulation of the flight environment can only be achieved by launching models at higher speeds. New gun technology is needed to accomplish this. Some concepts for advanced instrumentation and improved launch capabilities are discussed below.

Instrumentation

Obtaining high-quality data is a continuing problem for researchers in the ballistic range. In the past, experimenters have used many ingenious techniques to obtain quality data in this difficult environment. Today, even higher quality and a wider variety of data are needed, particularly in the area of CFD code calibration/validation. To date, most diagnostics employed in the range have been, of necessity, optical. Because the models are relatively small and the position of the model as it passes a measurement station cannot be predicted precisely, spatial resolution is sacrificed to ensure that the model is captured in the optics. Considerations of spatial resolution forces the experimenter to use the largest model practical. The uncertainty in the position of the model can be minimized by guiding it within a set of tracks, as is done at AEDC.[15] Naturally, this rules out aerodynamic force-and-moment determinations. The speed with which the model passes the measurement station requires submicrosecond exposure times to eliminate the effects of motion blur. Extremely powerful light sources, faster optics and more sensitive sensors are required. Recent advances in lasers, optics, and computational capability, generally, have not been employed in the ballistic range because of the recently ended period of reduced interest. In the following paragraphs, some of these advances will be touched upon as possible candidates to exploit in range instrumentation.

The accuracy to which aerodynamic coefficients can be determined is dependent on the accuracy to which the model position, orientation, and time-of-flight can be measured, and to the precision to which the data-reduction routine can match the measured trajectory. Advances in image processing offer the possibility of improving the accuracy to which we can measure the position and orientation of models. Time-of-flight resolution can be greatly improved by installation of modern data-acquisition equipment. Also improvements have been made in the data-reduction routines available for deducing aerodynamic coefficients. As an example, previous data-reduction methodology was capable of generating effective aerodynamic coefficients for single shots. Modern routines are capable of reducing data from multiple shots simultaneously and yielding the effect of angle of attack and velocity change on drag coefficient directly.[16] Work is proceeding to extend these routines to determine aerodynamics coefficients which exhibit hysteresis.

Flow-field structure data are typically obtained from shadowgraphs, but Schlieren systems are sometimes used. A holographic interferometry system is presently being used at the low-speed Air Force Armament Laboratory at Eglin AFB and such a system is being developed at Ames. These techniques give a two-dimensional image of the second, first, or zeroeth derivative of the density field that has been integrated over the optical path length. If the flow is axisymmetric, the experimental data can be inverted by the use of the Abel transformation. This is a time consuming process and much information and accuracy is lost in the transformation. If the density information is to be compared with computer solutions, it is better for the computer-generated density field to be converted into a simulated interferogram or Schlieren for comparison with the experimental data. All of these systems lose resolving capability at low air density, where chemical-kinetic phenomena are most important. Sharma and Park[17] state that, for a Schlieren system to be useful in the low-density regime, its contrast sensitivity must be increased by two orders of magnitude over present capabilities. They discuss ways to increase the contrast sensitivity of Schlieren systems by an order of magnitude. The resolution of the interferometer must be increased four-fold.

Presently at AEDC, model surface temperatures can be measured by observing the visible and infrared (IR) emission from the model surface material. In the AEDC system,[18] spatial resolution of 0.3 to 1.5 mm and temporal resolution of about 100 ns has been achieved by frontal imaging of a bluff body. Temperatures in a range of 1200 K to 5000 K can be measured to an accuracy of about ±150 K. Spatial resolution for the planform of the model continues to be a problem, especially in the IR where sensors are not fast. Advances in sensor technology will help in this area. Still, the major source of error in these systems is determination of the emissivity of the model material. Emissivity is a function of the condition and temperature of the surface, and the heating history. Thermographic phosphors, which have been developed for temperature measurement of engine parts[19] and do not depend on the emissivity of the material, may make it possible to measure lower surface temperatures more accurately than with present systems.

Because the model passes by the measurement station so rapidly usually only one measurement can be made at any one station with a given instrument. For this reason, measurement schemes which obtain data in two dimensions have been emphasized in the ballistic range. Obtaining two-dimensional images of the velocity, density, temperature, and species in the flow will be important, especially in the validation of CFD codes. Nonintrusive techniques have been devised to measure these quantities by use of laser absorption and laser induced fluorescence.[20-24] Many of these techniques obtain two-dimensional information by imaging onto CCD arrays or image-intensifier cameras. The low number densities characteristic of the hypervelocity regime, however, result in a low signal-to-noise ratio and this is the major problem that must be addressed. Advances in imaging technology can be used to improve many of the techniques that have been used in the past in the range, for instance, of the measurement of radiative heat transfer and spectra.

Onboard instrumentation can be very useful in measuring surface temperature, heat transfer, and pressure. Such measurements can serve as independent corroboration for measurements made with other instruments or provide a single absolute value to calibrate techniques that provide only relative information. The small model size restricts the number and sophistication of instruments that can be carried onboard. Also, the high acceleration loads experienced during launch provide severe restriction on the kinds of instruments that can be carried aboard the model. Previous systems employed radio transmitters to telemeter information out; at speeds in excess of 4 km/s, however, the shock wave in front of the model will ionize the air creating interference with the radio signal. A project under way at Ames is exploring ways around these problems.

Concerns about spatial resolution in optical diagnostics and the need to put instrumentation on board the model tend to drive model sizes larger. But these problems can also be solved by improvements in optical diagnostics or miniaturizing electronics. There is another, more important, reason for seeking larger model sizes. That is the desire to simulate as closely as possible the chemical kinetics of full-scale flows. In order to obtain the proper chemical kinetics, the correct enthalpy is required (by matching velocity) and the collision frequency between species (molecular and/or atomic) must match flight conditions. In compression regions, such as the stagnation region of a blunt body, where dissociation occurs, two-body collisions dominate the kinetics. This requires that the product of density and length scale, ρL, be matched. In an expansion region, such as a nozzle, where recombination occurs, three-body collisions play an important role in the kinetics. Matching the three-body collisions accurately requires that $\rho^2 L$ be matched. It may not be possible to achieve the proper chemical scaling in anything but a full-scale flight vehicle. For the purposes of CFD code validation, however, it is not important that both be matched exactly. It is important that the test be carried out under conditions where both two- and three-body collisions are important in order to test the chemistry in the code.

Launch Options

The most common model launchers for high-performance ballistic ranges at present are two-stage light-gas guns. The requirement to launch larger models at higher speeds dictate an improvement of the present launching capabilities of these guns. In this section, the operation and performance of the light-gas gun will be reviewed and potential increases in performance discussed. Several new technologies are under development that, theoretically, offer considerable increases in performance over the light-gas gun. The strengths and status of the most promising of these new technologies, namely the rail gun, coil gun, and "ramjet-in-tube" will be reviewed here.

The two-stage light-gas gun is the product of rapid development during the 1960s and gradual improvement in the intervening years. This relatively mature technology promises only small future improvements in velocity and moderate increases in launch mass unless much larger guns are built. A schematic of a conventional two-stage light-gas gun is shown in Fig. 12. The gun uses a charge of smokeless gunpowder to accelerate a heavy piston at moderate (usually less than 1 km/s) velocity down the pump tube. The piston, in turn, compresses a charge of propellant gas, usually hydrogen, to several kilobars pressure. Upon release by a burst diaphragm, the hydrogen propels the model to high speed in the launch tube. This moderately complex system provides a sufficiently wide selection of operation conditions to permit the launch of a wide range of

model mass to a moderate range of velocities with acceptable peak acceleration and jerk (the derivative of acceleration with respect to time). The chief drawbacks of the present technology are the small size of the model, the high peak accelerations (on the order of 150,000 to 500,000 g) and the maximum launch velocity (normally less than 10 km/s). In the past, in order to achieve increased performance in one of these areas, the other two must be sacrificed. At the General Motors Delco facility, masses of about 1 kg have been launched to 4 km/s in a 10-cm launch tube with peak accelerations of 150,000 g. A full scale-up of present technology to launch large masses to 8 km/s appears feasible.

A fundamental limitation on the present design is that all of the launch energy must be applied at the launch-tube breech; no workable scheme has been developed to permit staging of the guns in a manner contemplated for the electromagnetic guns and the ramjet-in-tube concept as described below. It is expected, however, that coupling an electromagnetic rail gun to the muzzle of a light-gas gun might permit each to operate in its optimal speed range. The electromagnetic rail gun works best at high speed because the load-dwell time at any point is short which minimizes damage to the rails.

During the last thirty years much effort has been expended in attempting to launch small projectiles to hypervelocities using rail guns. A typical distributed-energy-store railgun is shown schematically in Fig. 13.[25] A pair of rails, on opposite sides of the launch tube, complete an electrical circuit when an armature conductor connects them. The remaining surfaces completing the bore are insulators. When a current is forced to flow along one rail through the armature (metal or plasma at the base of the projectile) to the opposite rail and back to the power supply, the projectile is propelled by the resulting $J \times B$ force. As the projectile moves, the increasing resistive losses in the rails and diminishing energy in the supply source make it necessary to disconnect the initial source and connect the next supply source as indicated in the figure. The rail gun offers the advantage that launch accelerations can be tailored to the application at hand, and, in principle, high projectile speeds are possible. The performance of the rail gun at present appears to be limited to launching projectile masses of a few grams to speeds of 4 to 15 km/s.[26] One major difficulty preventing improvement of rail gun performance is confinement of the plasma armature. The strong repulsive forces between the rails tend to open a gap between the projectile and rail allowing plasma to escape. This plasma must be replenished by vaporizing material from the rails which results in severe rail erosion. The problems of rail erosion and high loading (leading to plasma escape) may prevent the rail gun from competing with the two-stage light-gas gun in the near future.

Another electromagnetic launcher under consideration which avoids the problem of plasma leakage is the coil gun.[27] The payload armature, a thin-walled aluminum sleeve, is suspended magnetically in a long series of solenoid coils as depicted in Fig. 14. The solenoids are excited by three-phase electrical power. The pitch length of the solenoid array is made progressively longer with increasing distance from breech to muzzle to provide accelerating magnetic waves which propel the projectile, even though the excitation frequency is diminishing rapidly. A complete coil gun may consist of several coil arrays placed in series, each array powered by its own pulse power alternator (compulsator) to achieve hypervelocity performance. The coil gun offers significant advantages over the rail gun in propelling large projectiles; however, efforts to develop the coil gun for high performance are in their infancy. There are severe difficulties in using the coil gun to launch large and fragile payloads. One of these is the extremely high external pressure tending to crush the lightweight armature. Another difficulty is the resistive heating of the armature. Ongoing efforts to develop coil guns for launching strong dense projectiles may succeed in overcoming the present obstacles and permit a major advance in size and performance for ballistic ranges.

Finally, a ramjet-in-tube concept[28] has been developed. In this concept, a finned projectile travels down a tube filled with a combustible gas mixture. The projectile acts as the ramjet centerbody and the tube wall acts as the ramjet cowl. In the thermally choked subsonic combustion mode, shown schematically in Fig. 15, a normal shock stands on the projectile, aft of the throat; and the flat base of the projectile acts as a flame-holding dump combustor. This mode of operation has been experimentally demonstrated at velocities from 0.7 to 2.3 km/s. Relatively constant accelerations of about 20,000 g have been achieved with a 50 gm, 38 mm projectile. Calculations indicate that drive modes using oblique detonation waves should operate effectively up to velocities of 7 to 10 km/s. The ramjet-in-tube concept offers relatively constant accelerations and can be scaled from projectile masses of grams to thousands of kilograms. Considerable development work must still be done before the ramjet-in-tube concept can be used in the ballistic range.

Conclusions

Future missions will require a better understanding of the aerothermodynamics of hypervelocity flight than presently exists. Because many future missions will fly in regimes outside of the simulation capability of present ground based facilities, CFD will be used increasingly in the design of these mission vehicles. Our ground-based facilities will be used extensively to develop a better understanding of the underlying physical phenomena involved and in calibrating the

CFD codes used to design these vehicles. The ballistic range is a very useful facility for hypervelocity testing. It is capable of excellent Mach number and enthalpy simulation over a wide range of conditions, has a very clean upstream chemistry, and small free stream disturbances. Also, there is no sting to interfere with study of the wake region. The models studied must be relatively small and simple, however, and data acquisition can be difficult. Examples of some of the data obtained in the range have been presented. By employing advanced diagnostics and developing the ability for onboard instrumentation in our present facilities, many of the questions concerning aerothermodynamic phenomena that exist today can be answered. Mission requirements and the need for onboard instrumentation require the development of guns that can launch larger projectiles to higher velocities than are presently attainable with light-gas guns. The operation and status of the main launching alternatives have been presented; however, none of these has reached the stage in its development where it can presently be considered as a replacement for the two-stage light-gas gun. The most conservative approach to achieve major increases in model size is thought to be enlargement of the light-gas gun. For the near term, it seems advisable to concentrate effort in the development of advanced instrumentation to enhance the capabilities of the existing ranges while keeping abreast of developments in alternative launch options.

Acknowledgment

In the conduct of this work, T. N. Canning was supported by NASA Grant NCC 2-504.

References

[1]National Commission on Space, Pioneering the Space Frontier, Bantam, New York, 1986.

[2]"National Aeronautical R&D Goads--Agenda for Achievement," Report, Executive Office of the President, Office of Science and Technology Policy, 1987.

[3]William, R. M., "National Aero-Space Plane: Technology for America's Future," Aerospace Am., Nov. 1986.

[4]Walberg, G. D., "A Survey of Aeroassisted Orbital Transfer," J. Spacecraft Rockets, Vol. 22, No. 1, 1985.

[5]Jones, J. J., "The Rationale for an Aeroassisted Flight Experiment," AIAA Paper 87-1508, June 1986.

[6]"Ballistic Range Technology," AGARDograph No. 138 (ed. Canning, T. N., Seiff, A., and James, C. S.)

[7]Intieri, P. F. and Kirk, D. B., "High-Speed Aerodynamics of Several Blunt-Cone Configurations," J. Spacecraft and Rockets, Vol. 24, No. 2, March-April 1987, pp. 127-132.

[8]James, C. S., "Observations of Turbulent-Burst Geometry and Growth in Supersonic Flow," NACA TN 4235, 1958.

[9]Compton, D. L. and Cooper, D. M., "Free-Flight Measurement of Stagnation-Point Convective Heat Transfer at Velocities to 41,000 ft/sec," NASA TN D-2871, June 1965.

[10]Craig, R. G. and Davy, W. C., "Absolute Radiometers for Use in Ballistic-Range and Shock-Tube Experiments," NASA TN D-5360, Oct. 1969.

[11]Page, W. A. and Arnold, J. O., "Shock Layer Radiation of Blunt Bodies at Reentry Velocities," NASA TR R-193, 1964.

[12]St. Pierre, C., "The Visible Emissions from 0.5 Inch Hypervelocity Models Measured with a Moving Target Scan Monochromator," CARDE TM AB-59, 1960.

[13]Reis, V. H., "Oscillator Strengths for the N_2 Second Positive and N_2^+ First Negative Systems from Observations of Shock Layers About Hypersonic Projectiles," J. Quant. Spectrosc. Radiant Transfer, Vol. 4, pp. 783-792.

[14]Whiting, E. E., "Determination of Mars Atmospheric Composition by Shock-Layer Radiometry During a Probe Experiment," AIAA Thermophys. Spec. Conf., New Orleans, Apr. 17-20, 1967.

[15]AEDC Test Facilities Handbook, March 1984, Air Force Systems Command, USAF.

[16]Winchenbach, G. L., Uselton, R. L., Hathaway, W. H., and Chelekis, R. M., "Free-Flight and Wind-Tunnel Data for a Generic Fighter Configuration," J. Aircraft, Vol. 21, No. 1, Jan. 1984, pp. t-13.

[17]Sharma, S. C. and Park, C., "A Survey of Simulation and Diagnostic Techniques for Hypersonic Nonequilibrium Flows," AIAA Paper 87-0406, Jan. 1987.

[18]Hendrix, R. E. and Dugger, P. H., "Role of High-Speed Photography in the Testing Capabilities of the Arnold Engineering Development Center (AEDC) Range and Track Facilities," Proc. 15th Int. Congress on High Speed Photography and Photonics, SPIE, Vol. 348, San Diego, CA, Aug. 1982.

[19]Noel, B. W., Allison, S. W., Beshears, D. L., Cates, M. R., Borella, H. M., Franks, L. A., Iverson, C. E., Lutz, S. S., Marshall, M. B., Turley, W. D., Dowell, L. J., Gillies, G. T., and Lutz, W. N., "Evaluating and Testing Thermographic Phosphors for Turbine-Engine Temperature Measurement," AIAA Paper 87-1761, June-July 1987.

[20]Kychakoff, G., Howe, R. D., and Hanson, R. K., "Quantitative Flow Visualization Technique for Measurements in Combustion Gases," Applied Optics, Vol. 23, No. 5, March 1984, pp. 704-712.

[21]Cattolica, R. and Vosen, S., "Combustion-Torch Ignition: Fluorescence Imaging of OH Concentration," Comb. Flame, Vol. 68, No. 3, June 1987, pp. 267-281.

[22]Miles, R. B., Connors, J. J., Howard, P. J., Markovitz, E. C., and Roth, G. J., "Proposed Single-Pulse Two-Dimensional Temperature and Density Measurements of Oxygen and Air," Optics Letters, Vol. 13, No. 3, March 1988, pp. 195-198.

[23]Chang, A. Y., Rea, E. C., and Hanson, R. K., "Temperature Measurements in Shock Tubes Using a Laser-Based Absorption Technique," Applied Optics, Vol. 26, No. 5, March 1987, pp. 885-891.

[24]Gross, K. P. McKenzie, R. L., and Logan, P., "Measurements of Temperature, Density, Pressure, and their Fluctuations in Supersonic Turbulence Using Laser-Induced Fluorescence," Exp. in Fluids, Vol. 5, No. 6, 1987, pp. 372-380.

[25]Haight, C. H. and Tower, M. M., "Distributed Energy Store (DES) Railgun Development," IEEE Transactions on Magnetics, Vol. Mag-22, No. 6, Nov. 1986.

[26]Hawke, R. S., Nellis, W. J., Newman, G. H., Rego, J., and Susoeff, A. R., "Summary of EM Launcher Experiments Performed at LLNL," IEEE Transactions on Magnetics, Vol. Mag-22, No. 6, Nov. 1986.

[27]Driga, M. D., Weldon, W. F., and Woodson, H. H., "Electromagnetic Induction Launchers," IEEE Transactions on Magnetics, Vol. Mag-22, No. 6, Nov. 1986.

[28]Hertzberg, A., Bruckner, A. P., and Bogdanoff, D. W., "The Ram Accelerator: A New Chemical Method for Accelerating Projectiles to Ultrahigh Velocities," AIAA J., to be published Feb. 1988.

LOW LIFT TO DRAG RATIO

AEROASSISTED ORBITAL TRANSFER VEHICLE

HIGH LIFT TO DRAG RATIO

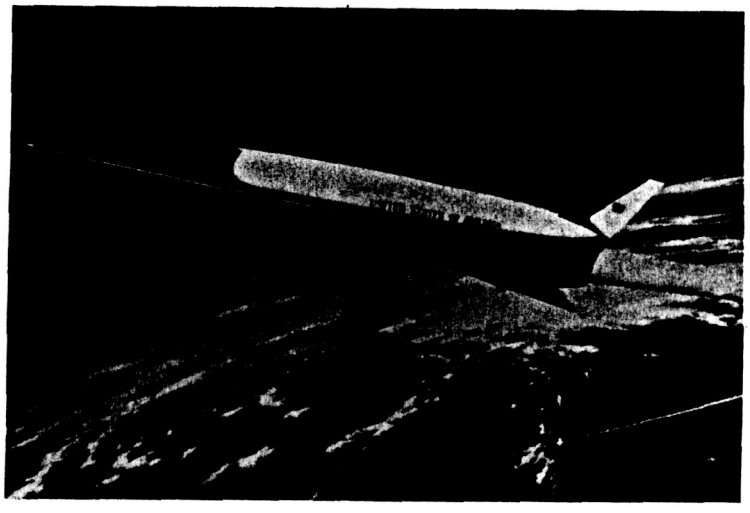

SINGLE-STATE-TO-ORBIT WITH AIR BREATHING PROPULSION

Fig. 1 Typical advanced hypersonic vehicle configurations.

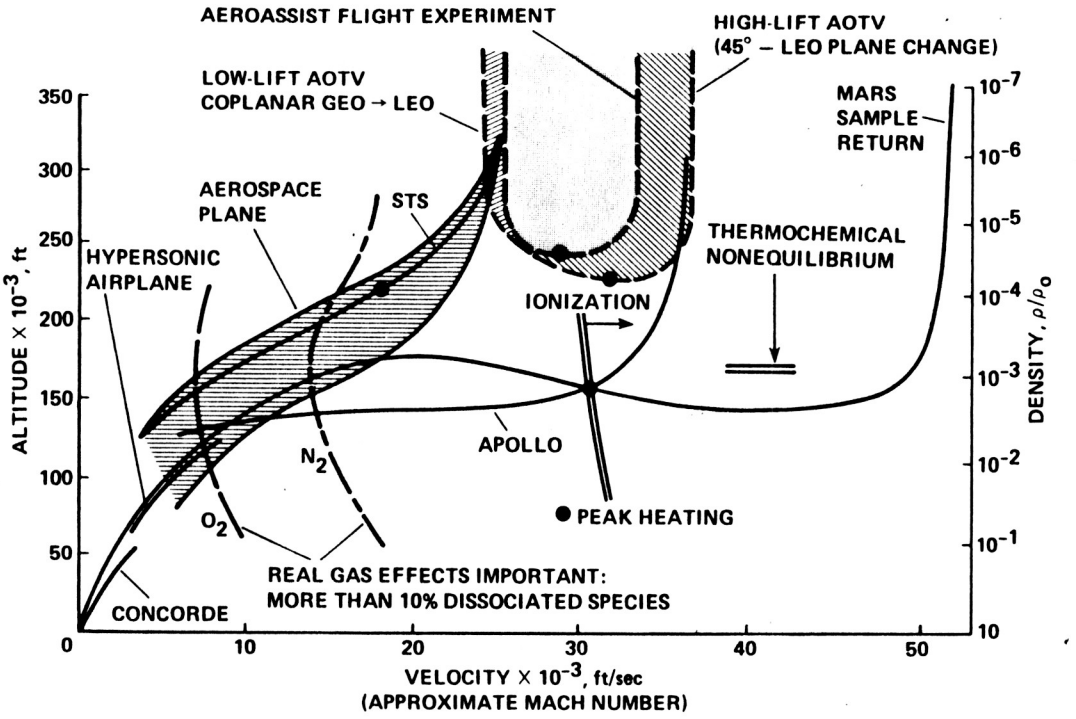

Fig. 2 The hypervelocity flight environment.

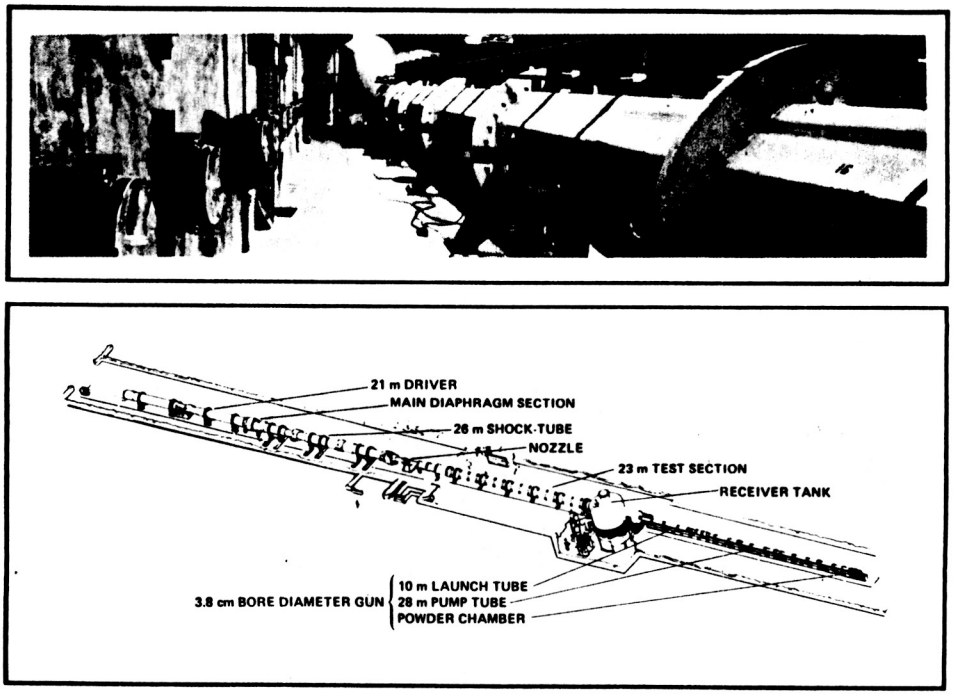

Fig. 3 The NASA Ames hypervelocity free-flight aerodynamic facility.

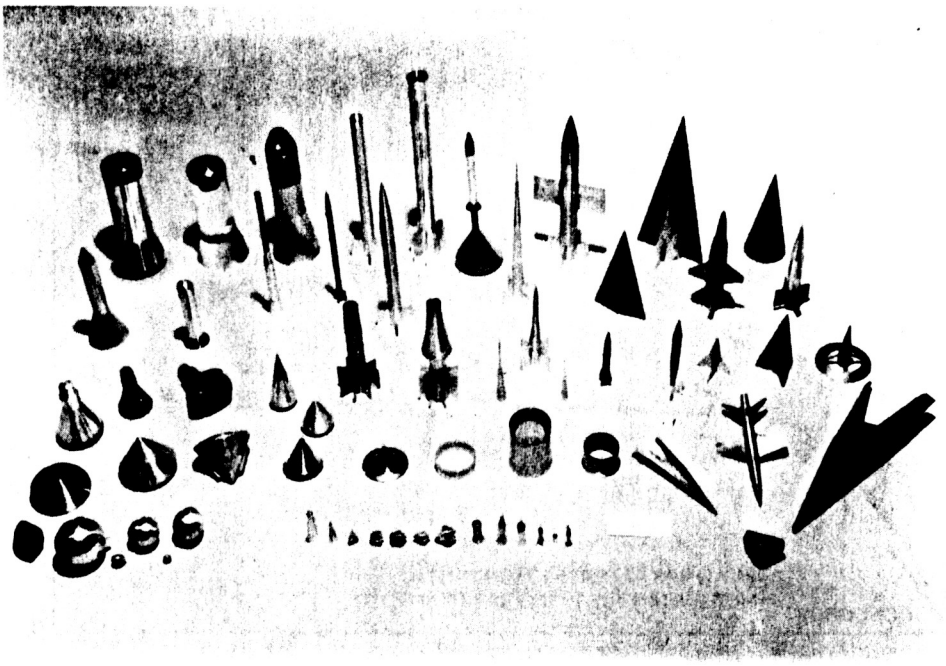

Fig. 4 Some typical ballistic range models.

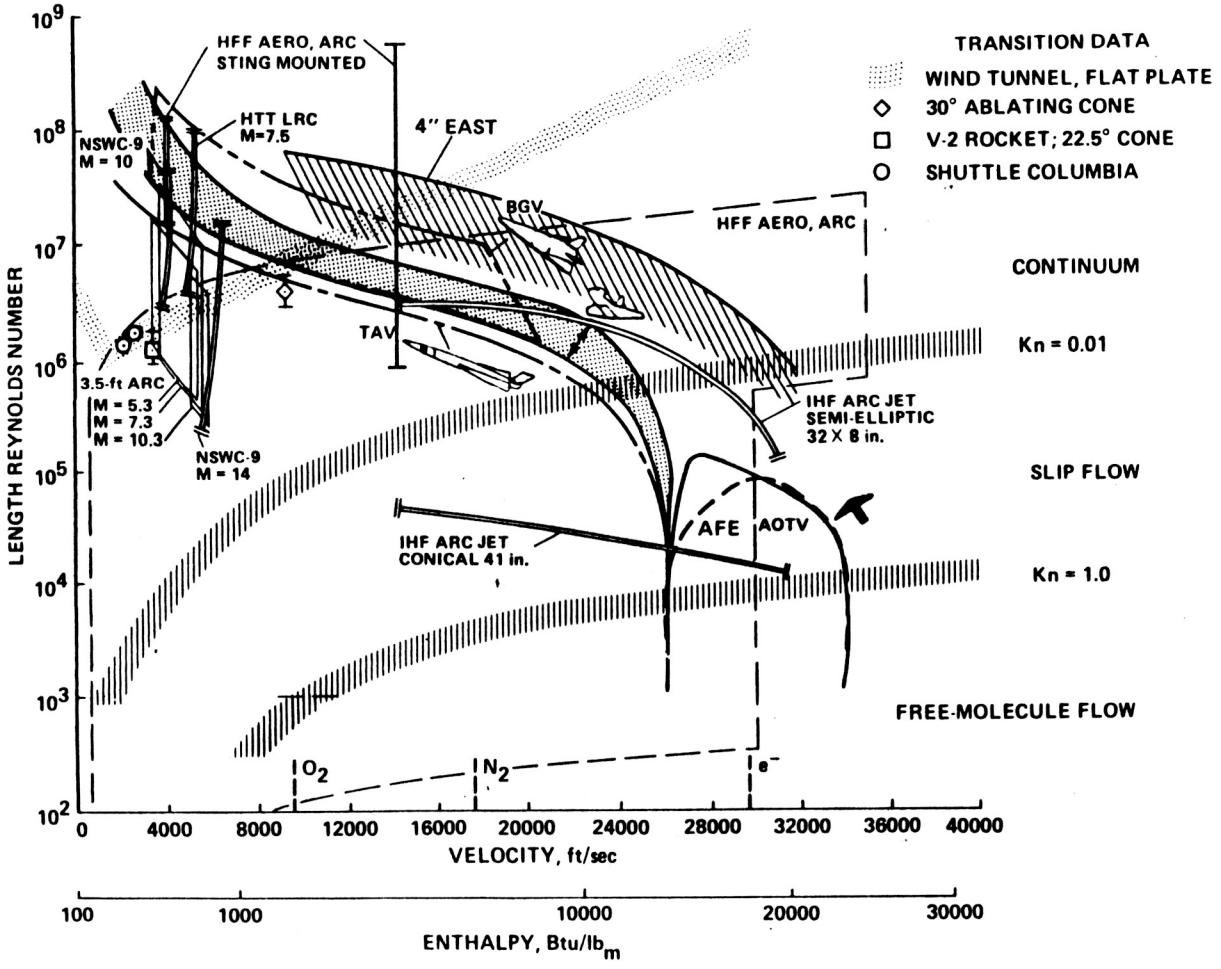

Fig. 5 Simulation capability of hypervelocity facilities.

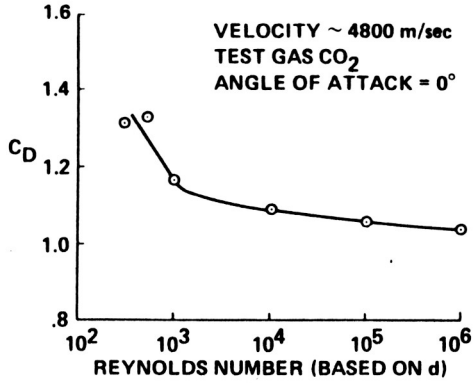

Fig. 6 Drag coefficient versus Reynolds number for Pioneer-Venus probe model.

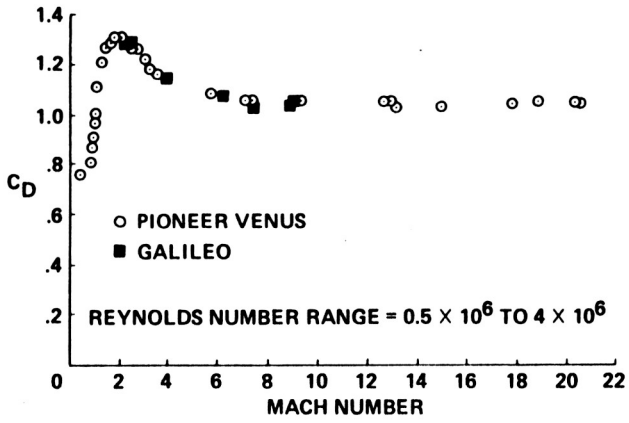

Fig. 7 Drag coefficient versus Mach number for Pioneer-Venus probe model.

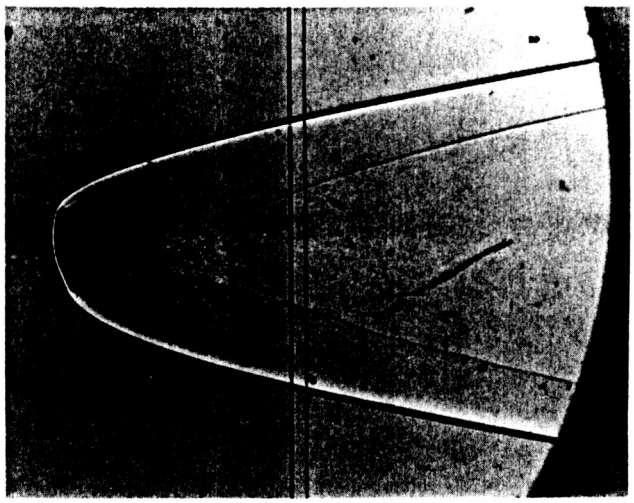

Fig. 8 Shadowgraph showing flow field structure about simple AOTV model.

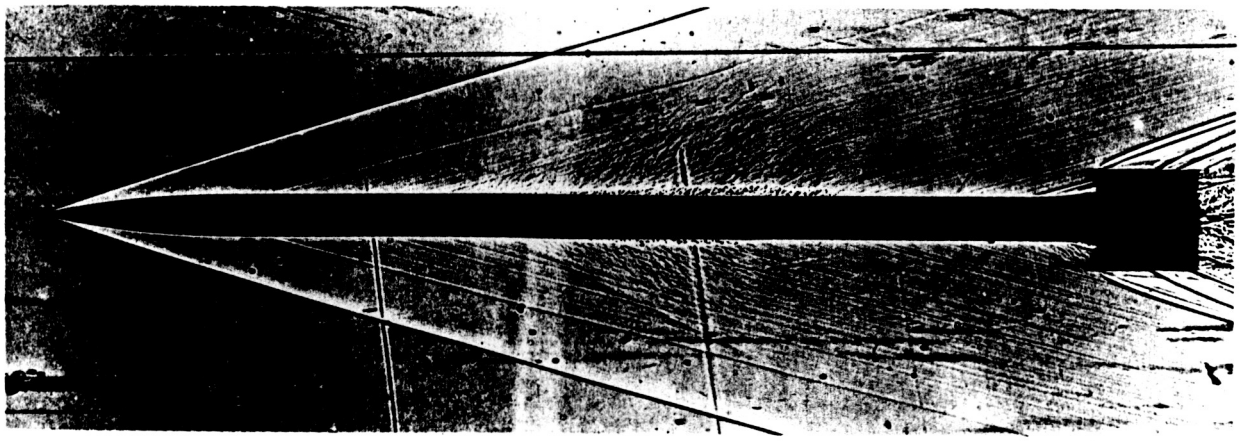

Fig. 9 Shadowgraph showing transition on a pencil model at Mach 3.9.

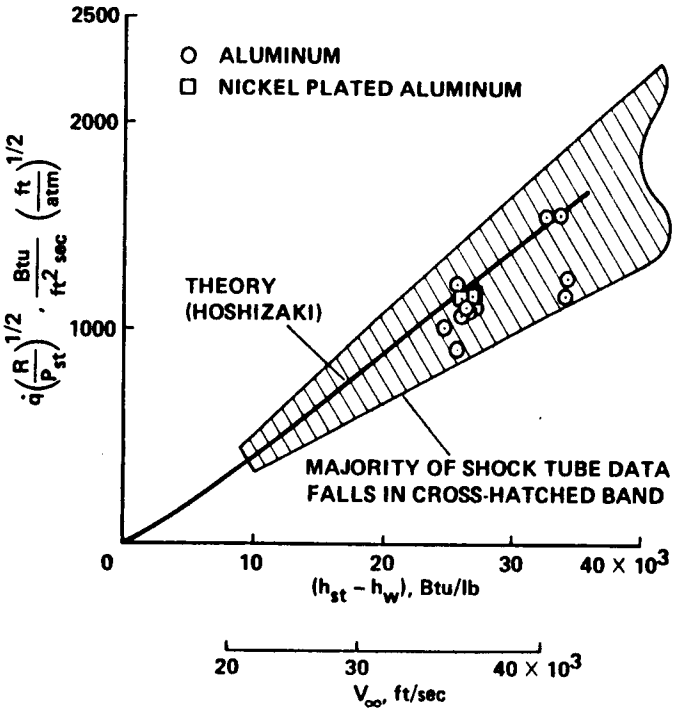

Fig. 10 Convective heating data for hemispheres.

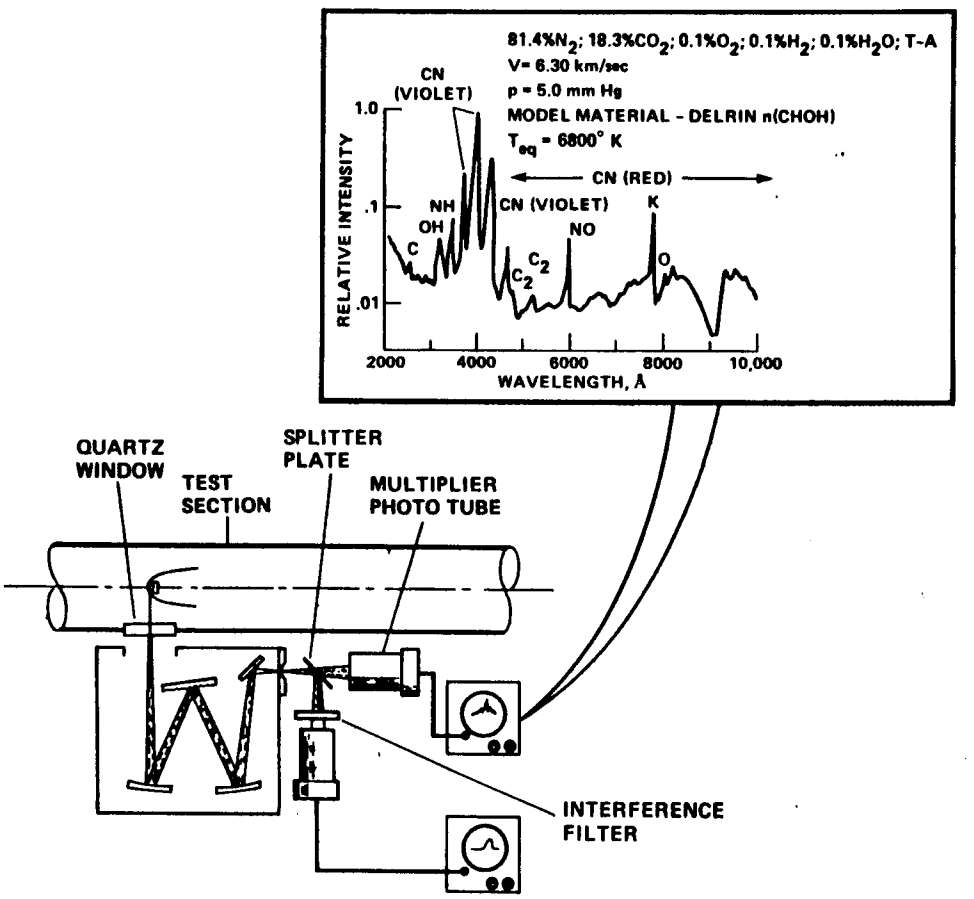

Fig. 11 Time-of-flight scanning spectrometer and typical data obtained from a free-flight ballistic range test.

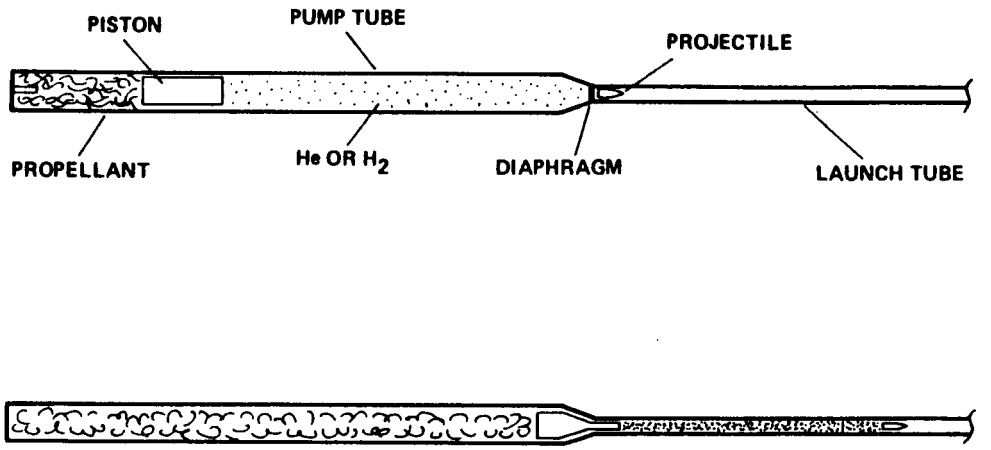

Fig. 12 Conventional two-stage light-gas gun.

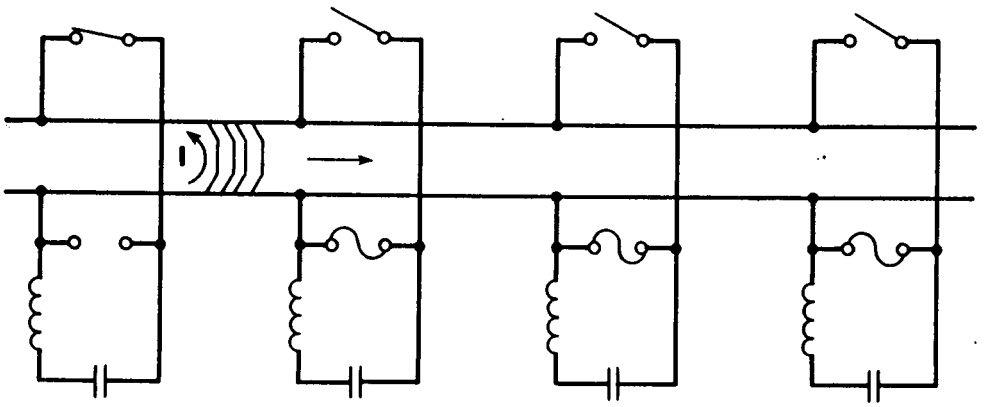

Fig. 13 Distributed energy store rail gun.

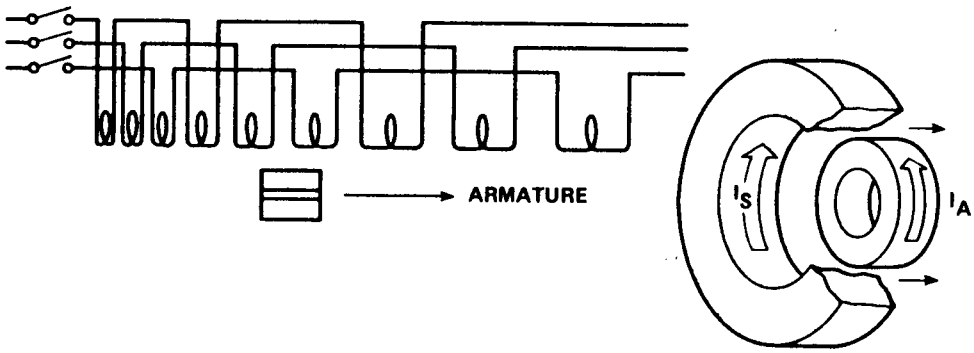

Fig. 14 Coil gun.

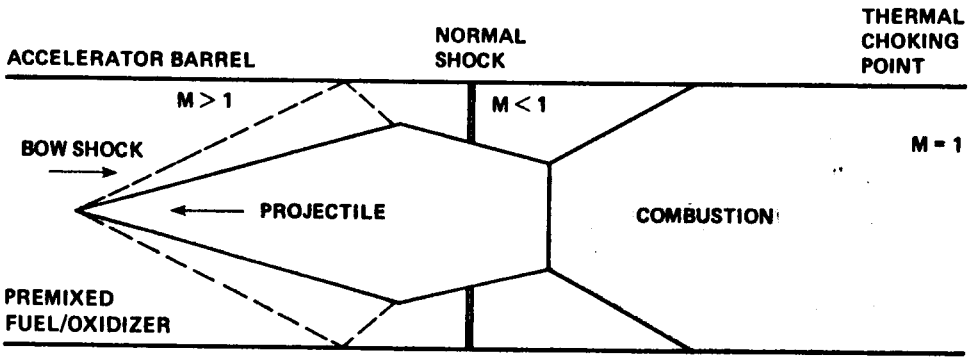

Fig. 15 Ramjet-in-tube concept (thermally choked subsonic mode of operation).